Proceedings of the 10th International Conference on Civil Structural and Transportation Engineering (ICCSTE 2025)
July, 2025 | Imperial College London Conference Center, London, United Kingdom
Paper No. ICCSTE 361
DOI: 10.11159/iccste25.361

Influence of LRB Isolators on Accelerations and Shear Forces in an Eight-Story Building with Shear Walls in Comas, Lima, Peru

Lenin Bendezú [1], Enrique Durand[1], Paul Awoyera[2]
[1]Universidad Privada de Trujillo, Perú
[2]Department of Civil Engineering, Prince Mohammad Bin Fahd University,
Al Khobar, Saudi Arabia.
lenin.bendezu@uprit.edu.pe; enrique.durand@uprit.edu.pe; pawoyera@pmu.edu.sa

Abstract - Earthquakes are one of the leading causes of material losses and loss of human life worldwide. For this reason, ensuring the safety of buildings is of utmost importance. An effective solution to mitigate these risks is base isolation systems, a technology designed to reduce the impact of seismic movements on building structures. This study examines the influence of LRB (Lead Rubber Bearings) devices on the structural behavior in terms of accelerations and shear forces in an eight-story building, utilizing Etabs v22 software. The study compares structural performance through a nonlinear time-history analysis of a fixed base building against the same building equipped with a base isolation system. The results for the base isolated building demonstrate a reduction and a more uniform distribution of floor accelerations, which improves the stability of the building contents. Shear forces were significantly reduced by 72.76%, highlighting the effective flexibility of the implemented isolation system. Additionally, the energy dissipated by the LRB system achieved an efficiency of 76.5%. These findings confirm those reported in other studies and emphasize the importance of considering the implementation of these seismic protection systems in housing projects located in high seismic risk areas, such as the district of Comas, Lima, Peru.

***Keywords*:** base isolation system, seismic isolator LRB, accelerations, shear forces, dissipated energy.

1. Introduction

The capital of Peru, Lima, is experiencing rapid growth in the construction of multifamily buildings. Specifically, in the district of Comas, located north of the capital, notable projects such as Ciudad Sol El Retablo and Los Parques de Comas are being developed in the former Collique aerodrome area. However, there is an underlying concern regarding safety in the event of a major earthquake. Although real estate projects adhering to national standards such as NTE E.060 (Reinforced Concrete) and NTE E.030 (Seismic-Resistant Design) are executed rigorously, these standards only ensure that structures will not collapse during a severe earthquake but do not prevent significant structural damage that could lead to substantial economic losses and even fatalities. According to NTE E.030 (Seismic-Resistant Design), Comas is located in Seismic Zone 4 of Peru, which signifies a high potential for large-magnitude earthquakes (M > 6.2). Thus, it is imperative for residential buildings in this district to incorporate some form of seismic protection system, such as base isolation employing elastomeric devices. Currently, buildings in Comas, including multifamily housing and critical structures like the Sergio Bernales hospital, lack any seismic protection system. Only new district level and national level hospital projects are mandated to include these protection systems. This situation poses a significant risk to the safety of inhabitants and the contents of buildings during high intensity seismic events.

To enhance the understanding of base isolation systems, various studies have been conducted to enrich the literature on Lead Rubber Bearings (LRBs). One such study proposed a model for LRB isolators incorporating a hardening correction to achieve a more precise characterization of their nonlinear behavior under large deformations, enabling a more realistic assessment during high-magnitude earthquakes [1]. Another research effort introduced an optimized method for designing LRB seismic isolation systems using the Grasshopper Optimization Algorithm. The study evaluated performance in 5- and 10-story building models under different seismic conditions [2]. In experimental scenarios, a modified LRB isolator was proposed, incorporating vertical holes filled with a mixture of sand and rubber particles, creating a three-dimensional vibration isolator that effectively addresses vibrations caused by trains and earthquakes [3]. Presently, various types of seismic isolators offer different performance levels during seismic events. Some authors in the literature compare the performance of LRB and FPS (Friction Pendulum System) isolators in irregular buildings with 3, 7, and 10 stories through nonlinear dynamic analyses [4]. They also evaluated differences in maximum responses between LRB and FPS isolators

under various earthquake simulations and seismic intensity levels, drawing conclusions on their efficiency in terms of displacements, accelerations, base shear, and other variables [5].

In this context, an evaluation is proposed to analyze the influence of LRB isolation devices on the structural behavior of a building, specifically regarding floor accelerations and shear forces. This study is expected to contribute to understanding the performance of isolated structures and their application in future multifamily building projects in Comas, Lima, Peru, and other global projects.

2. Methodology

2.1. Conventional fixed base building

Our study begins with the modeling of an eight-story slender building, approximately 93.00 m² in area, using the Etabs v22 software. The structure features a shear wall system, non-symmetrical dimensions, irregular characteristics, and a certain degree of torsion (Fig. 1).

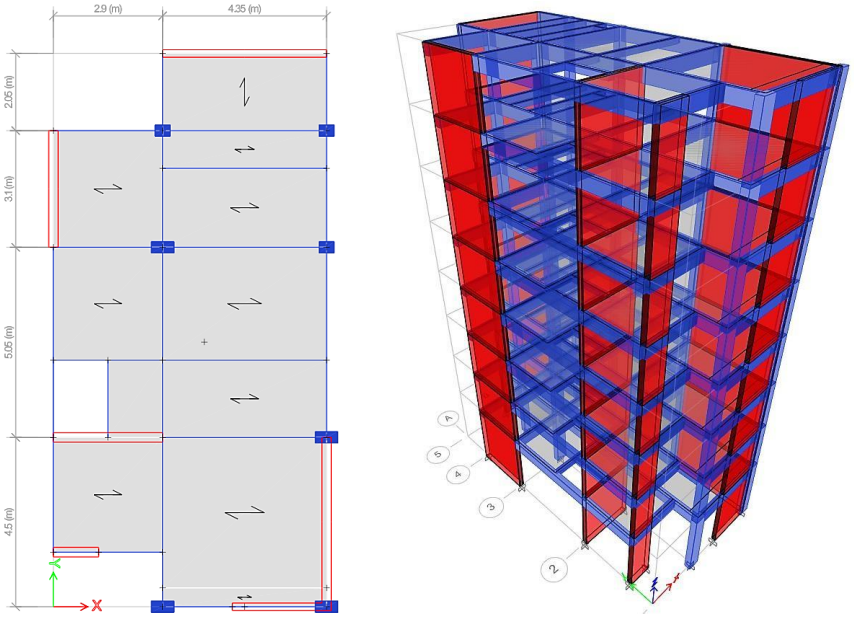

(a) (b)

Fig. 1: (a) Plan view of the fixed base building. (b) Modeling of the fixed base building.

The seismic parameters of the building under study are shown in Table 1. Additionally, the three primary periods for the structure were T_X=0.54 s, T_Y=0.53 s and T_{RZ}=0.31 s (Annex Fig. 12). These periods serve as the basis for determining the target period T_{obj} and the maximum translational displacement D_M of the isolation system. Furthermore, the model underwent a nonlinear time-history analysis in Etabs v22 in accordance with the NTE E.030 Seismic-Resistant Design code. For the analysis procedure, three seismic records were used, filtered and scaled to the target spectrum corresponding to the design earthquake with R=1 (Fig.3).

Table 1: Seismic parameters of the fixed base structure.

Z	**U**	**S**	**T_P**	**T_L**	**R_0**
0.45 g	1	1.0	0.40 s	2.5 s	6

2.2. Isolated base building

The base isolation system, with a height of 2 meters, was modeled in Etabs v22 and integrated into the original building model (Fig. 2). For the design of the LRB isolators, 16 isolators were considered, corresponding to the interaction of each isolator with the capital that supports the columns and structural walls of the conventional building. The service loads transferred to each isolator were divided into three ranges to avoid using the same type of LRB isolator throughout the system. This approach aimed to achieve a better distribution of the isolators' effective stiffnesses within the isolation system. Consequently, three LRB isolators were designed for each range of values (maximum, medium, and minimum). The geometric and dynamic properties of the three designed isolators are summarized in Table 2.

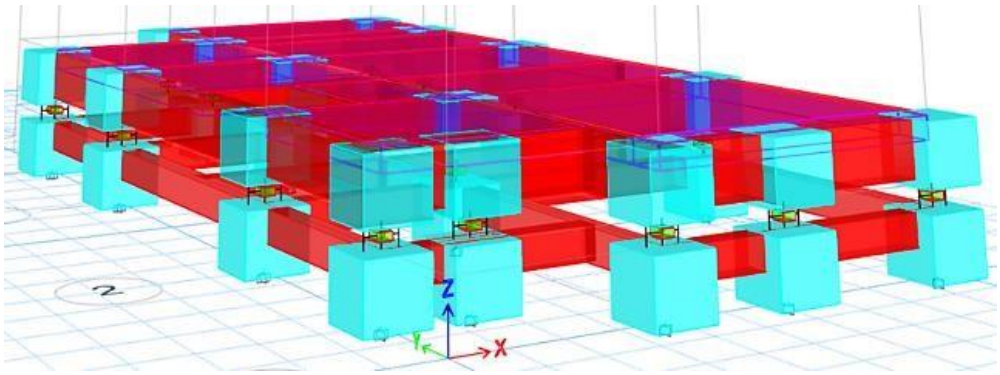

Fig. 2: Isolation system of the building.

Table 2: Nominal geometric and dynamic properties of the isolators.

Item	Symbol	Maximum	Average	Minimum	Units
Axial load on the isolator	P_{ais}	110	80	60	tonf
Isolator geometry					
Isolator diameter	D_{ais}	0.45	0.4	0.35	m
Lead core diameter	D_p	0.09	0.08	0.07	m
Rubber height	h_c	0.2	0.2	0.2	m
Rubber sheet thickness	t_{lc}	0.009	0.009	0.009	m
Steel sheet thickness	t_{la}	0.002	0.002	0.002	m
Coupling steel plate thickness	t_{paa}	0.0254	0.0254	0.0254	m
Insulator height		0.3	0.3	0.3	m
Dynamic properties					
Post-yield stiffness	K_d	54.49	43.06	32.96	tonf/m
Elastic stiffness	K_e	544.92	430.55	329.64	tonf/m
Characteristic force	Q_d	6.49	5.13	3.93	tonf
Yield force	F_y	7.21	5.7	4.36	tonf
Effective stiffness	K_{ef}	75.87	59.94	45.89	tonf/m
Energy dissipated in cycle	EDC	6.59	5.21	3.99	tonf.m
Yield displacement	d_y	0.05	0.05	0.05	m
Yield ratio	r	0.1	0.1	0.1	
Horizontal damping coefficient	C_h	9.06	7.16	5.48	tonf.s/m
Vertical stiffness	K_v	32692.96	21343.51	13046.41	tonf/m
Vertical damping coefficient	C_v	12.11	8.35	5.65	tonf.s/m

To verify the isolator design, the period T_M and damping β_M of the entire system were calculated based on the values obtained for each isolator. These were then compared to the target period T_{obj} and target damping β_{obj} in the Ec. (1). For the design to meet acceptable nominal values, the system's period and damping had to approximately match the target values in the Ec. (2).

$$\beta_{M=15.4\%} \cong \beta_{obj=15.0\%} \tag{1}$$

$$T_M = 2.2\ s\ \cong T_{obj} = 2.5\ s \cong T_{ETABS} = 2.3\ s \tag{2}$$

After integrating the isolation system, the linear and nonlinear properties of the LRB isolators were input into the analysis software. Subsequently, a nonlinear time-history dynamic analysis was performed following the requirements of NTE E.031 Seismic Isolation. For this analysis, seven seismic records were used, which were filtered and scaled to the target spectrum, corresponding to the Maximum Considered Earthquake (MCE) (Fig. 3)

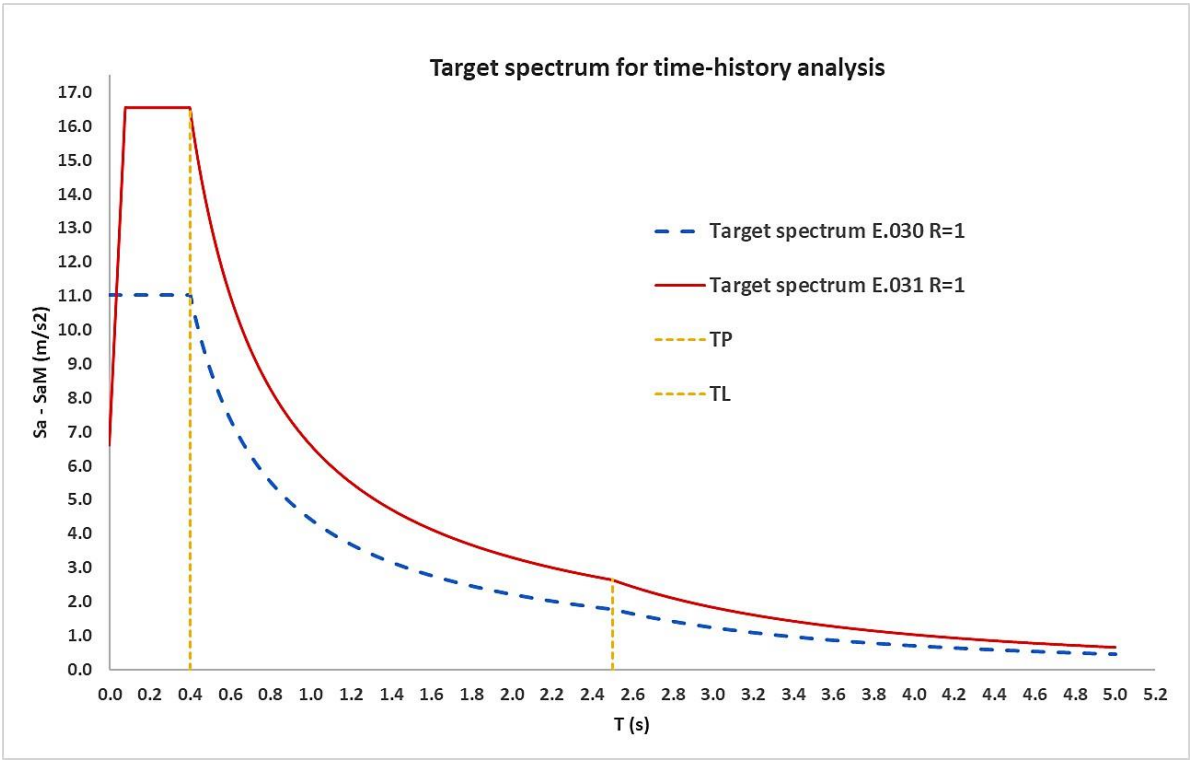

Fig. 3: Target spectra for the time-history analysis.

3. Results, analysis, and interpretation

The results presented below correspond to the nonlinear time-history analysis conducted for both the fixed base and base isolated buildings. Maximum average values for each study response (accelerations and shear forces) in each seismic analysis direction are presented and compared.

3.1. Maximum Average Accelerations

Floor accelerations measure the response of each level to seismic forces. These accelerations result from the interaction of the structure's mass, stiffness, and damping properties with ground motion. (Table 3).

Table 3: Average accelerations in the XX and YY directions.

	Earthquake XX		Earthquake YY	
Story	**Fixed Base a(m/s2)**	**Isolated Base a(m/s2)**	**Fixed Base a(m/s2)**	**Isolated Base a(m/s2)**
Story 8	24.10	5.89	14.82	6.60
Story 7	18.55	4.32	11.62	4.74
Story 6	14.70	3.03	9.68	3.11
Story 5	12.51	2.28	8.87	2.68
Story 4	10.78	2.09	8.42	2.47
Story 3	8.94	2.52	7.76	2.86
Story 2	6.60	3.26	6.09	3.50
Story 1	5.00	4.31	4.76	4.31
Base	4.36	5.82	4.58	5.81

In the XX direction, as indicated in Table 3 and Fig. 4(a), the accelerations in the fixed base building progressively increase with height. The maximum acceleration recorded for the fixed base structure was 24.10 m/s², while for the base isolated structure, it was significantly lower, reaching only 5.89 m/s². Moreover, the accelerations in the base isolated structure were much smaller and more uniform (less dispersed) compared to those in the fixed base structure. This clearly demonstrates that the lateral forces generated by earthquakes were significantly reduced due to the implementation of the isolation system.

In the YY direction, as shown in Table 3 and Fig. 4(b), a similar trend is observed: accelerations in the fixed base building increase progressively with height. The maximum acceleration recorded for the fixed base structure was 14.82 m/s², whereas for the base isolated structure, it was significantly lower, reaching only 6.60 m/s². Similarly, the accelerations in the base isolated structure were much smaller and more uniform (less dispersed) compared to those in the fixed base structure. This clearly demonstrates that the lateral forces generated by earthquakes were significantly reduced thanks to the implementation of the isolation system.

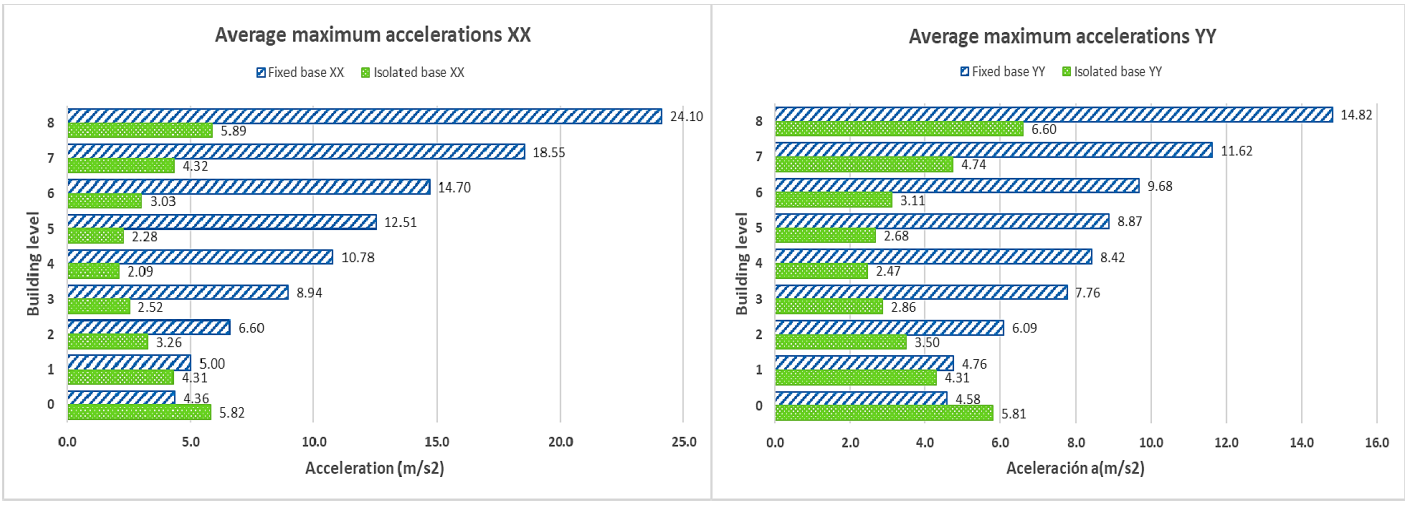

(a) (b)

Fig. 4: Graphs of average acceleration in the XX and YY directions.

3.2. Maximum average shear forces

Shear forces represent the horizontal forces accumulated in each floor due to the accelerations generated by an earthquake (Table 4).

Table 4: Average shear forces in the XX and YY directions.

	Earthquake XX		Earthquake YY	
Story	**Fixed Base VX**	**Isolated Base VX**	**Fixed Base VY**	**Isolated Base VY**
Story 8	124.90	32.80	108.90	39.90
Story 7	237.30	66.00	211.90	87.80
Story 6	312.40	92.10	290.00	117.50
Story 5	369.60	110.30	348.10	132.90
Story 4	418.80	120.80	402.80	140.00
Story 3	468.50	127.60	451.00	142.20
Story 2	509.60	138.30	490.30	157.30
Story 1	529.70	144.30	520.90	168.10
Base	0.00	111.60	0.00	100.60

In the XX direction, based on the data presented in Table 4 and Fig. 5(a), the base shear acting at the first level of the fixed base structure was 529.7 tonf, whereas for the base isolated structure, it was significantly reduced to 144.3 tonf, representing a 72.76% reduction. This remarkable decrease in base shear is consistently observed across all floors of the structure, demonstrating the effectiveness of the implemented isolation system. The system's flexibility allows for better dissipation of seismic forces, reducing their impact on the structure.

In the YY direction, as per the data in Table 4 and Fig. 5(b), the base shear acting at the first level of the fixed base structure was 520.9 tonf, while for the base isolated structure, it decreased significantly to 168.1 tonf, representing a 67.73% reduction. This substantial reduction in base shear is consistently observed across all floors, further confirming the effectiveness of the isolation system. Its flexibility allows for better dissipation of seismic forces, significantly mitigating their impact on the structure.

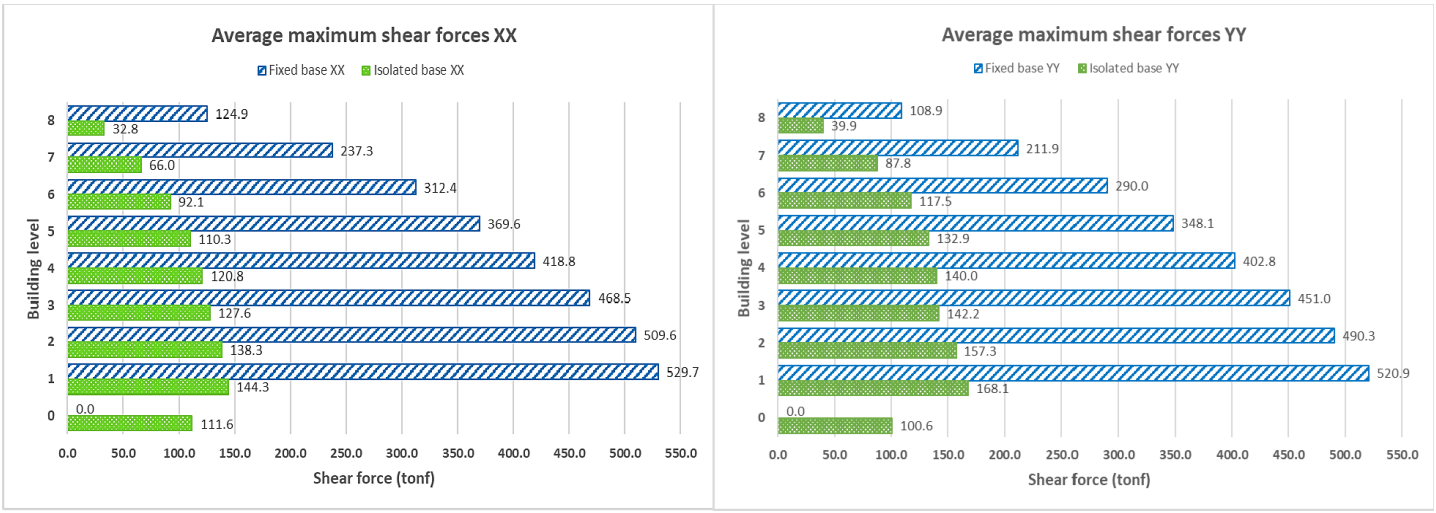

(a) (b)

Fig. 5: Graphs of average shear forces in the XX and YY directions.

3.3. Energy balance of the isolation system

On one hand, in the case of the fixed base building, 100% of the seismic energy entering the system is absorbed and dissipated directly by the structure itself. If the material exceeds its elastic range, this dissipation results in structural damage. On the other hand, in buildings with base isolation systems, the isolators dissipate energy through hysteretic cycles generated by their deformation during an earthquake. According to Table 5 and Fig. 6, the system comprising 16 LRB isolators dissipated 76.5% of the seismic energy entering the system, while the remaining percentage was absorbed and dissipated by the structure itself.

Table 5: Input energy and energy dissipated by the isolation system.

Earthquake	**Horizontal component**	**Input energy (tonf-m)**	**Isolation system (tonf-m)**	**Dissipated energy (%)**
Ancash 6.6 Mb	EW	477.5	377.3	79.02%
	NS	477.5	377.3	
Barranca 8.1 M_W	EW	431.4	347.2	80.50%
	NS	431.4	347.2	
Cañete 6 Mb	EW	357.7	255.0	71.30%
	NS	357.7	255.0	
Lima 6.2 Mb	EW	515.2	386.2	75.00%
	NS	515.2	386.2	
Lima 6.6 Mb	EW	546.0	414.7	75.90%
	NS	546.0	414.7	
Moyobamba 7.2 M_L	EW	705.5	539.5	76.50%
	NS	705.5	539.5	
Pisco 7.0 M_L	EW	634.3	492.0	77.60%
	NS	634.3	492.0	
Averages		**524.48**	**401.63**	**76.50 %**

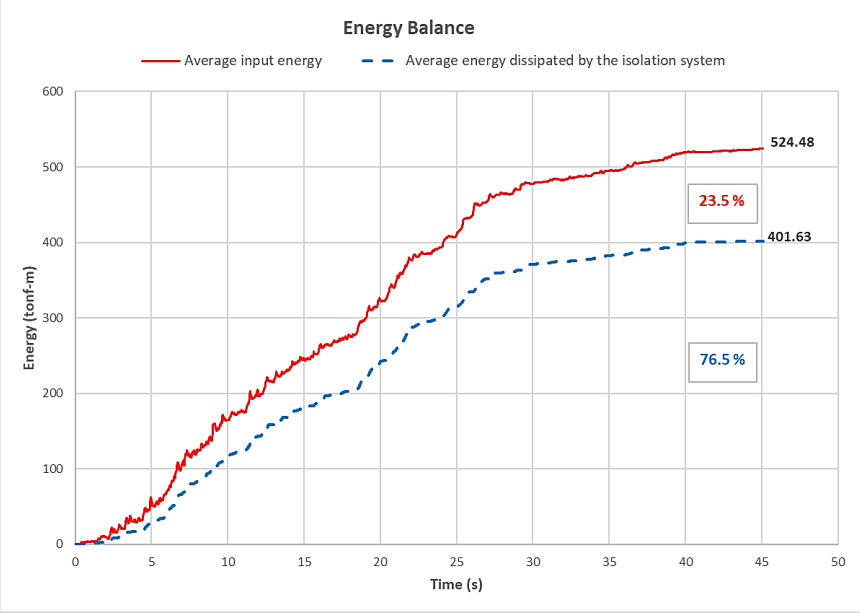

Fig. 6: Energy balance curves.

4. Conclusions

The maximum acceleration in the fixed base structure was recorded in the XX direction, at the top floor, reaching 24.10 m/s², whereas in the base isolated structure, also in the XX direction and at the top floor, it was significantly lower, with a value of 5.89 m/s². Not only were the accelerations in the base isolated structure considerably lower, but they were also more uniform (less dispersed) compared to those in the fixed base structure. This clearly demonstrates that the implemented isolation system effectively reduces lateral forces generated by seismic events.

Regarding base shear, the maximum reduction occurred in the XX direction, with a percentage decrease of 72.76%. These results highlight a remarkable reduction in shear forces for the base isolated structure, confirming the efficiency of the flexibility provided by the isolation system. The significantly lower shear forces suggest that the base isolated structure is considerably relieved from lateral loads compared to the fixed-base structure.

The isolation system, composed of 16 LRB isolators, dissipated 76.5% of the total seismic energy entering the system, while the remaining percentage was absorbed and dissipated by the structure itself.

Based on previous studies, strategies could be explored to further enhance this performance. One possibility would be to combine LRB isolators with other types, such as NRB (Natural Rubber Bearings) or sliders. Another option would be to implement more flexible structural configurations in fixed base buildings, such as incorporating frame structural systems.

Acknowledgments

We express our gratitude to the Universidad Privada de Trujillo for its commitment to promoting and supporting scientific research, contributing to the strengthening and advancement of engineering in Peru.

A la Dirección de Investigación de la Universidad Privada de Trujillo por el apoyo brindado para realización de este trabajo de investigación a través del incentivo 2025-1.

References

[1] M. Chen, W. Liu, H. Xu, and Q. Zhang, "Improved seismic response prediction of isolated structures using hardening correction in a novel LRB model," *Journal of Building Engineering*, vol. 76, Oct. 2023, doi: 10.1016/j.jobe.2023.107123.

[2] F. Mehri, S. Mollaei, E. N. Farsangi, M. Babaei, and F. Ghahramanic, "Application of a Novel Optimization Algorithm in Design of Lead Rubber Bearing Isolation Systems for Seismic Rehabilitation of Building Structures," *International Journal of Engineering, Transactions A: Basics*, vol. 36, no. 3, pp. 594–603, Mar. 2023, doi: 10.5829/ije.2023.36.03c.20.

[3] T. Sheng, G. bin Liu, X. cheng Bian, W. xing Shi, and Y. Chen, "Development of a three-directional vibration isolator for buildings subject to metro- and earthquake-induced vibrations," *Eng Struct*, vol. 252, Feb. 2022, doi: 10.1016/j.engstruct.2021.113576.

[4] M. R. Shiravand, H. Ketabdari, and M. Rasouli, "Optimum arrangement investigation of LRB and FPS isolators for seismic response control in irregular buildings," *Structures*, vol. 39, pp. 1031–1044, May 2022, doi: 10.1016/j.istruc.2022.03.070.

[5] A. S. Vibhute, S. D. Bharti, M. K. Shrimali, and T. K. Datta, "Performance evaluation of FPS and LRB isolated frames under main and aftershocks of an earthquake," *Structures*, vol. 44, pp. 1532–1545, Oct. 2022, doi: 10.1016/j.istruc.2022.08.082.